

## Supplementary Information

### End-of-life MoS<sub>2</sub>-enabled device and material transformation in landfill leachate and their effects on the landfill microbiome

*Indu Venu Sabaraya*<sup>1†</sup>, *Xintong Li*<sup>2</sup>, *François Perreault*<sup>3</sup>, *Andrei Dolocan*<sup>4</sup>, *Jean Anne C.*

*Incorvia*<sup>2</sup>, *Mary Jo Kirisits*<sup>1</sup>, *Navid B. Saleh*<sup>1,\*</sup>

<sup>1</sup>Department of Civil, Architectural and Environmental Engineering, The University of Texas at  
Austin, Austin, TX 78712

<sup>2</sup>Department of Electrical and Computer Engineering, The University of Texas at Austin, Austin,  
TX 78712

<sup>3</sup>School of Sustainable Engineering and the Built Environment, Arizona State University,  
Tempe, AZ 85281

<sup>4</sup>Texas Materials Institute, The University of Texas at Austin, Austin, TX 78712

<sup>†</sup>Current Affiliation: Semiconductor Process Engineer, Micron Technology Inc., Boise, ID

\*Corresponding author: Navid B. Saleh; email: [navid.saleh@utexas.edu](mailto:navid.saleh@utexas.edu)

## **Summary of Supplementary Information**

- Number of pages: 15
- Number of tables: 2
- Number of figures: 5

## 1. R source code to process microbial DNA data

```
# Reference for code: https://joey711.github.io/phyloseq/import-data.html
# From raw data, format the following files:
# 1. As CSV: OTU or species table: Column 1 as species number or OTU number;
Remaining columns are sample data
# 2. As CSV: Taxonomy table: Column 1 as species number or OTU number;
Remaining columns are tax level (e.g., family, genus, phyla, etc.)
# 3. As CSV: Sample table: Column 1 with same sample names as the header row
in OTU table, and columns with sample variables (Leachate age, sampling time,
MoS2 concentration)

# Import the above CSV Files
OTUMAT <- read.csv(
  <PATH for File 1>,
  row.names = 1,
  check.names = FALSE
)
TAXMAT <- read.csv(
  <PATH for File 2>,
  row.names = 1,
  check.names = FALSE
)
s1 <- read.csv(
  <PATH for File 3>,
  row.names = 1,
  check.names = FALSE
)

# Format the imported files as OTU and TAX table with the phloseq package
# To install package and dependencies:
https://joey711.github.io/phyloseq/install.html
library("phyloseq")

OTU <- otu_table(OTUMAT, taxa_are_rows = TRUE)
TAX <- tax_table(TAXMAT)
sampledata <- sample_data(s1)

# To extract the sample information
Age <- sampledata$LeachateAge
SamplingTime <- sampledata$SampleTime
Concentration <- sampledata$Conc

# combine OTU and TAX using phyloseq
physeq <- phyloseq(OTU, TAX, sampledata)

# Create a random phylogenetic tree with the ape package, and add it to your
dataset.
# Match the tip labels to the values in OTU_table.
library("ape")
random_tree <- rtree(ntaxa(physeq),
  rooted = TRUE,
  tip.label = taxa_names(physeq)
)
```

```

# Merge by adding the new data components to the existing phyloseq by using
merge_phyloseq.
physeq1 <- merge_phyloseq(physeq, random_tree)
physeq1

# Import libraries for UNIFRAC Data Processing: Page 4 - https://cran.r-
project.org/web/packages/GUniFrac/GUniFrac.pdf
library(vegan)
library(GUniFrac)
library(ade4)
library(pairwiseAdonis)

unifrac <- GUniFrac(t(OTU), random_tree, alpha = c(0, 0.5, 1))$unifrac

dw <- unifrac[, , "d_1"] # Weighted UniFrac
du <- unifrac[, , "d_UW"] # Unweighted UniFrac
dv <- unifrac[, , "d_VAW"] # Variance adjusted weighted UniFrac
d0 <- unifrac[, , "d_0"] # GUniFrac with alpha 0
d5 <- unifrac[, , "d_0.5"] # GUniFrac with alpha 0.5

# PERMANOVA Analyses
adonis(unifrac[, , "d_0.5"] ~ Age+Concentration+SamplingTime)
#adonis(unifrac[, , "d_0.5"] ~ Age)
#adonis(unifrac[, , "d_0.5"] ~ Concentration)
#adonis(unifrac[, , "d_0.5"] ~ SamplingTime)

# Pairwise analyses in group with significant difference to compare samples
within group
pairwise.adonis(x=unifrac[, , "d_0.5"] factors = SamplingTime)
#pairwise.adonis(x=unifrac[, , "d_0.5"], factors = Age)
#pairwise.adonis(x=unifrac[, , "d_0.5"], factors = Concentration)

# Calculate PCoA based on UNIFRAC d5 distance matrix with k= number of
samples-1
# Cmdscale Documentation:
https://www.rdocumentation.org/packages/stats/versions/3.6.2/topics/cmdscale
# Use eigenvalues to calculate % of variation explained by first 2 principal
components
pcoa <- cmdscale(d5, k = 17, eig = TRUE, add = TRUE)

# Ecological Diversity Indices
# Function fisher.alpha estimates the parameter of Fisher's logarithmic
series
a <- fisher.alpha(t(OTU))
# Function diversity is Shannon or Shannon-Weaver (or Shannon-Wiener) index
is defined as  $H = -\sum p_i \log(b) p_i$ 
# Where  $p_i$  is the proportional abundance of species  $i$  and  $b$  is the base of
the logarithm.
b <- diversity(t(OTU))
# Function specnumber finds the number of species
c <- specnumber(t(OTU))

```

## **2. Nano-enabled Membrane preparation method**

First, the polysulfone support was fabricated by phase inversion via immersion precipitation as described in Justino et al (2021).<sup>1</sup> A polysulfone solution (16.3% w/w) was prepared in 1-methyl-2-pyrrolidinone (NMP, Sigma-Aldrich, St. Louis, MO) and degassed under vacuum before use. The polysulfone solution was spread on a glass plate using a casting knife (MTI Corporation, Richmond, CA), set to a thickness of 200  $\mu\text{m}$ . The polysulfone film was allowed to evaporate in ambient air for 30 s before immersion in a DI bath for phase inversion. The resulting membrane was cut to 9"  $\times$  5" pieces, rinsed, and immersed in DI water for 1 d to ensure complete solvent removal.

## **3. Aging of control membranes: Additional data**

### ***FTIR analyses of control membranes containing no MoS<sub>2</sub>***

Upon exposure to YL and ML over time, these characteristic peaks do not change over 2 months of exposure, indicating stability of the membranes against significant degradation in leachate during simple mechanical aging. Aggressive aging techniques such as UV-mediated accelerated aging may result in more pronounced changes to the surface functional groups and morphology.

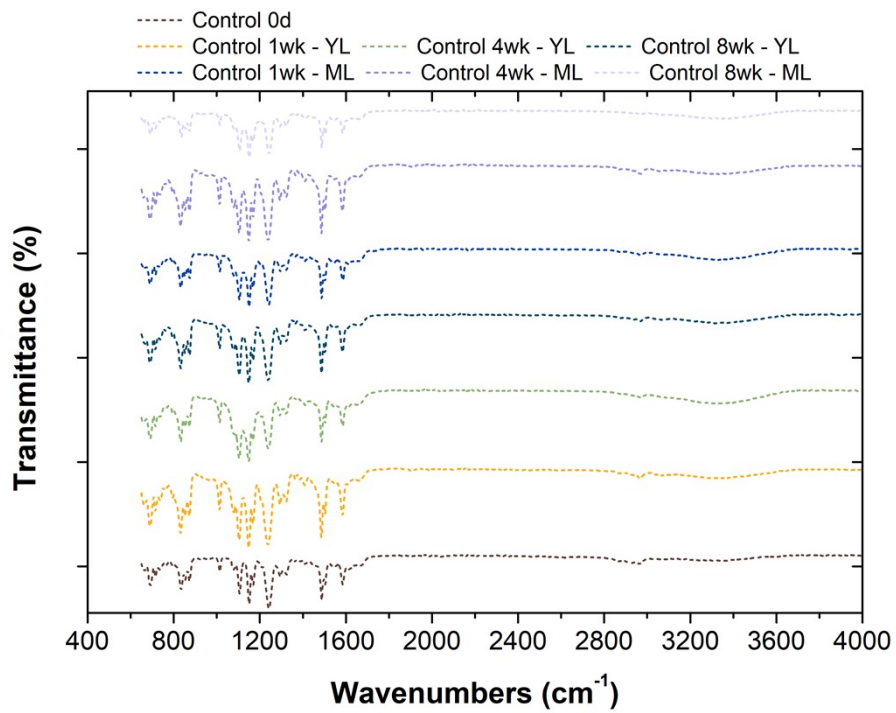


**Figure S1.** FTIR spectra of the control membranes in YL and ML over a period of 8 weeks.

*Additional SEM images at lower magnification*

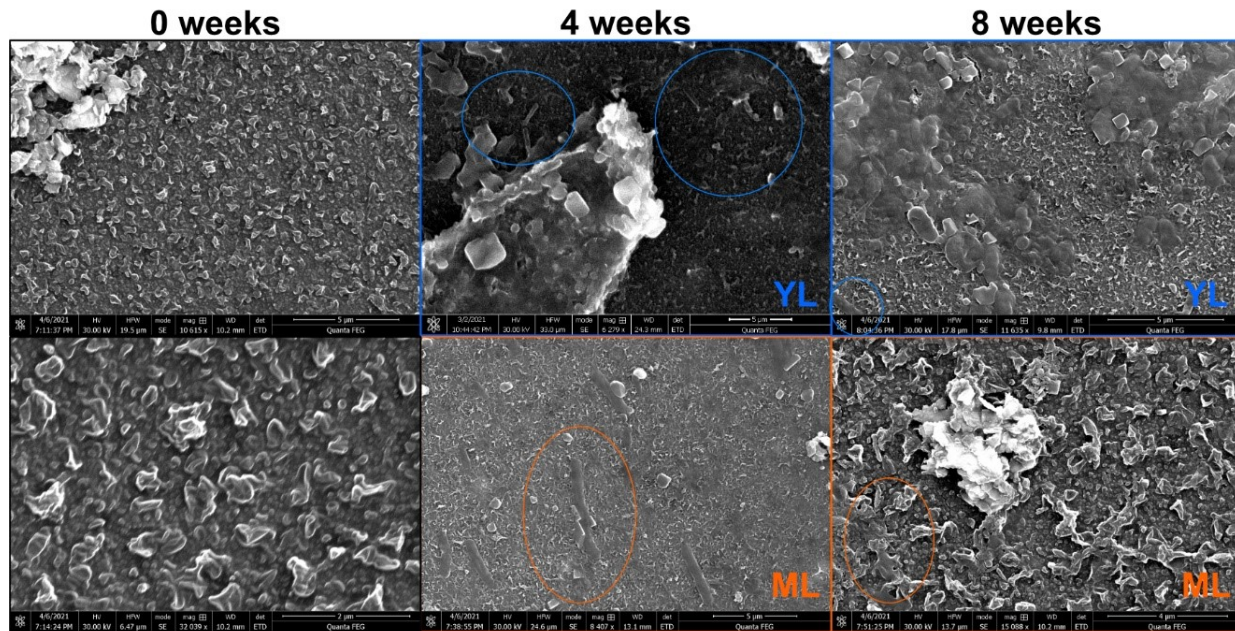


**Figure S2.** Additional SEM images at lower magnification (~10000x) of MoS<sub>2</sub> membranes aged over 8 weeks in YL and ML.

*ICP-OES data for tested samples*

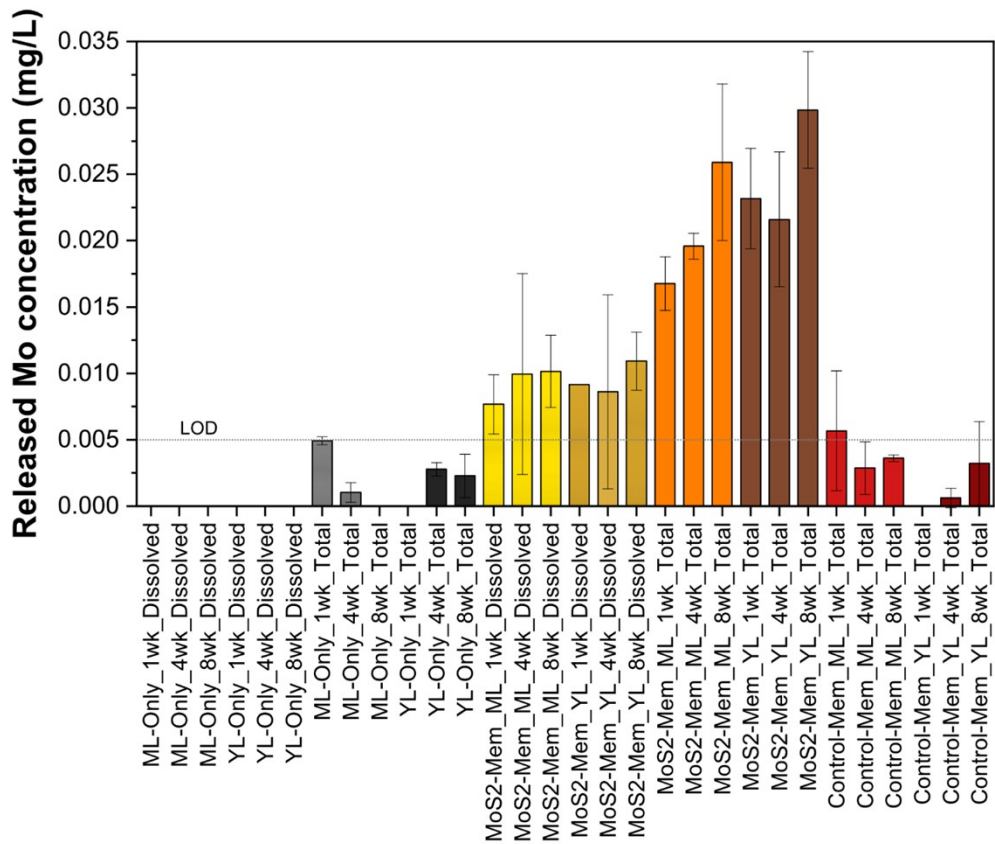


**Figure S3.** Concentration of molybdenum released (in mg/L) from membranes exposed to ML and YL over an exposure period of 8 weeks, measured by ICP-OES.



#### 4. Microbial DNA Analyses

##### *UniFrac Distances calculated for Bacterial OTUs at Alpha =0.5*

Here, ‘0’ indicates identical samples (green) and ‘1’ indicates that no branches in the phylogenetic tree are shared by the samples (red). Values shown in Table S1 are generated in the parameter d5 calculated from the source code shown in Document 1. This parameter is reported to be robust by controlling for the weight of more abundant lineages. The differences mainly correlate to time of exposure and not to MoS<sub>2</sub> concentration.

**Table S1.** UniFrac distances (d5) calculated using GUnifrac package in R.

	<b>M.0.0</b>	<b>M.1.0</b>	<b>M.100.0</b>	<b>M.0.4</b>	<b>M.1.4</b>	<b>M.100.4</b>	<b>M.0.8</b>	<b>M.1.8</b>	<b>M.100.8</b>
<b>M-0-0</b>	0.000	0.207	0.191	0.492	0.537	0.498	0.612	0.620	0.544
<b>M-1-0</b>	0.207	0.000	0.202	0.487	0.530	0.490	0.605	0.606	0.536
<b>M-100-0</b>	0.191	0.202	0.000	0.481	0.528	0.502	0.601	0.605	0.542
<b>M-0-4</b>	0.492	0.487	0.481	0.000	0.302	0.303	0.516	0.474	0.326
<b>M-1-4</b>	0.537	0.530	0.528	0.302	0.000	0.372	0.553	0.524	0.434
<b>M-100-4</b>	0.498	0.490	0.502	0.303	0.372	0.000	0.578	0.523	0.364
<b>M-0-8</b>	0.612	0.605	0.601	0.516	0.553	0.578	0.000	0.325	0.477
<b>M-1-8</b>	0.620	0.606	0.605	0.474	0.524	0.523	0.325	0.000	0.419
<b>M-100-8</b>	0.544	0.536	0.542	0.326	0.434	0.364	0.477	0.419	0.000
	<b>Y.0.0</b>	<b>Y.1.0</b>	<b>Y.100.0</b>	<b>Y.0.4</b>	<b>Y.1.4</b>	<b>Y.100.4</b>	<b>Y.0.8</b>	<b>Y.1.8</b>	<b>Y.100.8</b>
<b>Y-0-0</b>	0.000	0.108	0.140	0.369	0.389	0.404	0.431	0.442	0.454
<b>Y-1-0</b>	0.108	0.000	0.146	0.373	0.390	0.403	0.435	0.448	0.457
<b>Y-100-0</b>	0.140	0.146	0.000	0.385	0.401	0.414	0.447	0.456	0.460
<b>Y-0-4</b>	0.369	0.373	0.385	0.000	0.106	0.131	0.186	0.210	0.216
<b>Y-1-4</b>	0.389	0.390	0.401	0.106	0.000	0.141	0.175	0.199	0.218
<b>Y-100-4</b>	0.404	0.403	0.414	0.131	0.141	0.000	0.199	0.227	0.225
<b>Y-0-8</b>	0.431	0.435	0.447	0.186	0.175	0.199	0.000	0.144	0.171
<b>Y-1-8</b>	0.442	0.448	0.456	0.210	0.199	0.227	0.144	0.000	0.126
<b>Y-100-8</b>	0.454	0.457	0.460	0.216	0.218	0.225	0.171	0.126	0.000

**Ecological Diversity Indices**

Ecological diversity indices of the samples are shown below. The alpha diversity is relatively unchanged in the YL samples over time and with MoS<sub>2</sub> concentrations. The diversity values are lower in the ML samples as compared to the YL samples.

**Table S2.** Ecological diversity indices: Fisher Alpha, Shannon–Weaver Index and Number of Species for YL and ML samples exposed to 0, 1, and 100 mg/L MoS<sub>2</sub> over a period of 8 weeks.

Increasing time	ML with 0 mg/L MoS <sub>2</sub>			ML with 1 mg/L MoS <sub>2</sub>			ML with 100 mg/L MoS <sub>2</sub>			
	Time (week)	Fisher Alpha	Diversity	Species	Fisher Alpha	Diversity	Species	Fisher Alpha	Diversity	Species
	0	133.6	3.940	562	142.9	3.749	672	153.0	4.134	780
	4	149.6	4.429	766	137.9	4.273	721	135.3	3.886	710
	8	117.1	4.132	483	129.9	4.270	683	130.0	4.206	682
	YL with 0 mg/L MoS <sub>2</sub>			ML with 1 mg/L MoS <sub>2</sub>			ML with 100 mg/L MoS <sub>2</sub>			
	Time (week)	Fisher Alpha	Diversity	Species	Fisher Alpha	Diversity	Species	Fisher Alpha	Diversity	Species
	0	130.1	4.575	675	128.2	4.525	666	130.2	4.334	590
	4	141.5	4.641	729	141.2	4.594	725	142.0	4.640	726
	8	144.6	4.694	741	143.3	4.604	735	140.2	4.554	726

## 5. Archaeal Community Profiles

Euryarchaeota made up the most abundant Archaeal phylum in all samples, with an average relative abundance of 96%. Thus, to visualize potential differences more clearly, the community profile of Archaea at the order level is shown in **Figure S3 a-b**, with the associated PCoA plot and UniFrac distance matrices shown in **Figure S3 c-d**, respectively. As expected from published studies<sup>2</sup> on landfill microbiomes, methanogenic Archaea were predominantly present in ML samples, with high relative abundance of *Methanosarcinales*, *Methanococcales*, *Methanomicrobiales*, and *Methanobacteriales* in the community profiles. These hydrogenotrophic and mixotrophic Archaeal orders are important for landfill processes and functioning.<sup>3</sup> The Archaeal profiles are distinct between the YL and ML samples, right from 0 weeks. At 100 mg/L in both YL and ML, shifts in the microbial community are observed based on PCoA plots. However, majority of the shifts in the community profiles were again related to time rather than MoS<sub>2</sub> concentration for almost all cases.

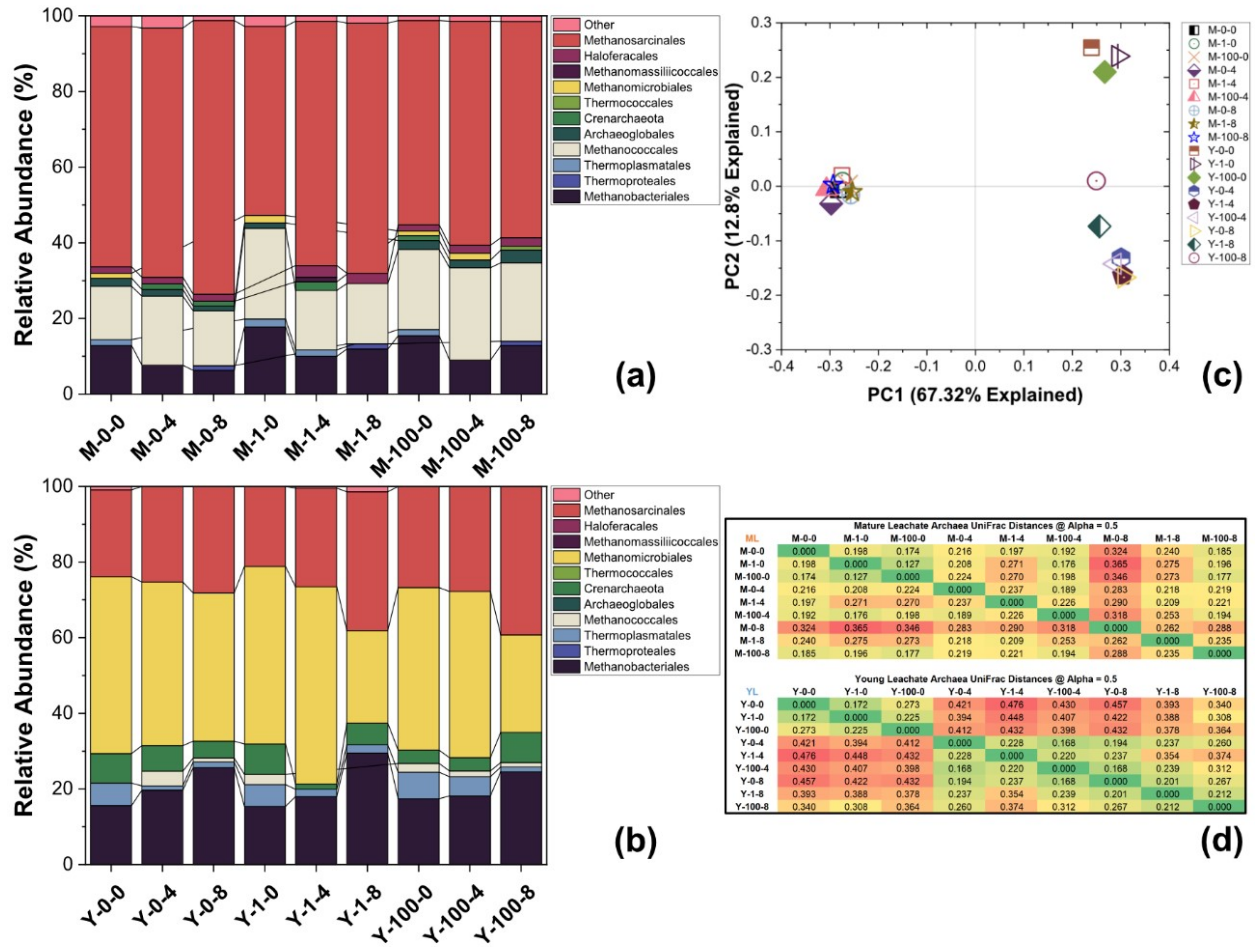


**Figure S4.** Relative abundance of Archaea at the Order level in (a) ML, and (b) YL in the presence of MoS<sub>2</sub>. Only operational taxonomic units comprising 1% or greater are shown. Sample names are read as: Y: young, M: Mature, First Number: MoS<sub>2</sub> concentration in mg/L, Second Number: Time in weeks. (c) PCoA plot for Archaeal OTUs. (d) UniFrac distance matrix for Archaeal OTUs.

## **6. Tolerance by pure culture strain *Pseudomonas putida***

The tolerance of a Gram-negative soil bacterium, *Pseudomonas putida* strain F1 (provided by Dr. Michael Hyman from North Carolina State University), to colloidal dispersions of TMDs (MoS<sub>2</sub> and Black Phosphorus, 90 mg/L aqueous dispersions, 2D Semiconductors, Scottsdale, AZ) was assessed. *P. putida* is selected because it is a common soil bacterium, has been used in bio-treatment of wastes<sup>4,5</sup>, and has been detected among soil and airborne<sup>6</sup> microorganisms in landfills. A freezer stock of *P. putida* F1 was created by inoculating a colony from the provided plate and overnight growth at 37 °C. A small aliquot of the grown bacteria was mixed with 50% glycerol and frozen at -80 °C.

The bacterial freezer stock was struck on a Luria Bertani (LB) agar plate and grown overnight at 30 °C. A single colony from the plate was then inoculated to LB medium and incubated at 30 °C in a shaker at 200 rpm for 18-24 h. This was sub-cultured in fresh LB medium and incubated at 30 °C until mid-exponential phase was achieved. A 20-μL aliquot of diluted TMD was added to 180 μL of the bacterial suspension on a microtiter plate to achieve final exposure concentrations of 0.1, 1 and 10 mg/L TMD. A control was prepared by adding 20 μL sterile phosphate-buffered saline (PBS) to the bacterial suspension. Exposure to the TMDs was conducted for 2 h. The samples were serially diluted, grown on LB agar plates, incubated for 12-16 h at 37 °C, and finally, colonies were enumerated by viable counts.

### ***MoS<sub>2</sub> tolerance by pure culture strain *P. putida****

The measured *P. putida* cell density upon a 2-hour exposure to three concentrations of MoS<sub>2</sub> and Black Phosphorus (BP) nanosheets is shown in **Figure S5**. Exposure to MoS<sub>2</sub> and BP from 0-10 mg/L results in minor decreases in cell density of *P. putida*. In the MoS<sub>2</sub> system, the

cell density decreases only approximately 36%, from  $(45.5 \pm 3.4) \times 10^5$  CFU/mL at 0 mg/L MoS<sub>2</sub> to  $(29 \pm 1.4) \times 10^5$  CFU/mL at 10 mg/L MoS<sub>2</sub>. A one-way ANOVA showed that there was at least 1 significant difference in the groups ( $F(3,12) = 25.32$ ,  $p = 1.78E-05$ ). Post-hoc Tukey-Kramer analysis showed that the control group (0 mg/L) was significantly different from the MoS<sub>2</sub>-containing (0.1, 1, 10 mg/L) groups at  $p < 0.05$ . Within the MoS<sub>2</sub>-containing groups, the 0.1 mg/L vs 1 mg/L and 1 mg/L vs 10 mg/L were not statistically significant at  $\alpha = 0.05$ . Another TMD of interest to recent electronic applications is black phosphorous (BP), which is a thermodynamically stable allotrope of the phosphorus element that forms a layered 2D structure. Phosphorus is an essential element for all microorganisms, being important for metabolism, membrane structure, and genetic information storage and transfer. Upon exposure to BP from 0-10 mg/L, the cell density decreases from  $(45.5 \pm 3.4) \times 10^5$  CFU/mL at 0 mg/L BP to approximately  $(28.7 \pm 2.5) \times 10^5$  CFU/mL at 10 mg/L BP. Exposure of environmentally-relevant bacterial densities (i.e.,  $10^5$  CFU/mL) to high MoS<sub>2</sub> or BP concentrations (i.e., higher than environmentally-relevant concentrations) decreased bacterial densities in a statistically significant fashion as compared to the control (0 mg/L nanomaterial); however, because the bacterial densities remained at the same order of magnitude (i.e.,  $10^5$  CFU/mL), we project that MoS<sub>2</sub> and BP would not exert substantial toxicities under environmentally-relevant nanomaterial exposures.

In comparison to the above values, the literature reports high silver nanoparticle (AgNP) toxicity to *P. putida*, with EC<sub>50</sub> values (i.e., effective concentration resulting in a 50 percent reduction) ranging from 0.16-13.4 µg/L total silver, through a combination of factors such as shape, size, coating, dissolution of Ag<sup>+</sup> (which is biocidal to bacteria).<sup>7</sup> Another study that studied the toxicity of pristine and aged AgNPs in urban wastewaters using a bioluminescent *P.*

*putida* species reported ion-based toxicity in the mg/L range, and decreased toxicity by aged AgNP samples that was attributed to Ag aggregation and complexation.<sup>8</sup>

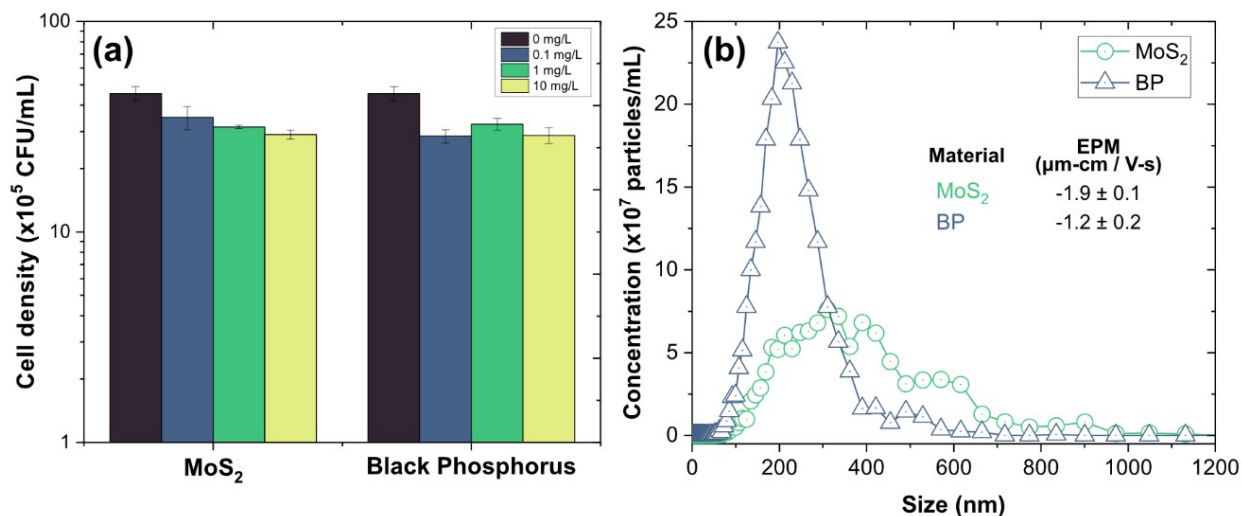


**Figure S5.** (a) Cell density of *P. putida*, following 2-h exposure to 0, 0.1, 1, and 10 mg/L of MoS<sub>2</sub> and Black Phosphorus (BP) nanosheets. Error bars represent the standard deviations of duplicate experiments, each consisting of two wells per treatment per experiment. (b) Particle size distribution of 10 mg/L suspensions of MoS<sub>2</sub> and BP nanosheets in 1X PBS. Average and standard deviation of the electrophoretic mobility of the nanosheets in 1X PBS also are provided.

A study by Yang et al.<sup>9</sup> demonstrated low toxicity of 2D MoS<sub>2</sub> to *Escherichia coli*. Exposure of *E. coli* DH5α to 20 mg/L exfoliated MoS<sub>2</sub> for 2 h resulted in a loss of cell viability of 60%, as compared to around 40% in the case of raw MoS<sub>2</sub> powder. Additionally, they also reported that aggregated MoS<sub>2</sub>, that were formerly well-exfoliated, exerted even less toxicity than did raw MoS<sub>2</sub> powder to the cells at all tested exposure times (2, 4, 6 h). Other reports on the toxicity of 2D TMDs also indicate that these materials exert less toxicity in their bulk (multilayer) form as compared to the few- or mono-layered forms.<sup>10</sup> It is thus suggested that the

nanosheet morphology (thin layers) and high surface area contribute to toxicity. In contrast, MoS<sub>2</sub> did not show an appreciable toxicity to lung cancer cells for an exposure period of 16 h with cell viability only decreasing by 30% for an exposure concentration of 12.5 mg/L.<sup>11</sup> However, Chng et al. reported that that fewer nanosheet layers (increased exfoliation) results in increased toxicity to human lung carcinoma epithelial cells when the MoS<sub>2</sub> dosage was high (>100 mg/L upon a 24-h exposure).<sup>12</sup> In a subset of data reported by Chng et al., dosages comparable to the present study (0-12.5 mg/L of MoS<sub>2</sub>) resulted in cell viability above 85% at all tested levels of exfoliation. In general, MoS<sub>2</sub> appears to have low toxicity to cells at concentrations that would be considered 'high' in environmental systems. However, the effect of these thin materials over long timescales and continuous input (such as accumulating ENM-enabled wastes in MSW landfills) could become relevant as they might exert stresses (e.g., membrane stress) on microorganisms in the leachate over time.



## References

- (1) Justino, N. M.; Vicentini, D. S.; Ranjbari, K.; Bellier, M.; Nogueira, D. J.; Matias, W. G.; Perreault, F. Nanoparticle-Templated Polyamide Membranes for Improved Biofouling Resistance. *Environ. Sci. Nano* **2021**, *8* (2), 565–579. <https://doi.org/10.1039/d0en01101k>.
- (2) Zhao, R.; Liu, J.; Feng, J.; Li, X.; Li, B. Microbial Community Composition and Metabolic Functions in Landfill Leachate from Different Landfills of China. *Sci. Total Environ.* **2021**. <https://doi.org/10.1016/j.scitotenv.2020.144861>.
- (3) Song, L.; Wang, Y.; Zhao, H.; Long, D. T. Composition of Bacterial and Archaeal Communities during Landfill Refuse Decomposition Processes. *Microbiol. Res.* **2015**, *181*, 105–111. <https://doi.org/10.1016/j.micres.2015.04.009>.
- (4) Michalska, J.; Piński, A.; Zur, J.; Mroziak, A. Analysis of the Bioaugmentation Potential of *Pseudomonas Putida* OR45a and *Pseudomonas Putida* KB3 in the Sequencing Batch Reactors Fed with the Phenolic Landfill Leachate. *Water (Switzerland)* **2020**, *12* (3). <https://doi.org/10.3390/w12030906>.
- (5) Zuo, Z.; Gong, T.; Che, Y.; Liu, R.; Xu, P.; Jiang, H.; Qiao, C.; Song, C.; Yang, C. Engineering *Pseudomonas Putida* KT2440 for Simultaneous Degradation of Organophosphates and Pyrethroids and Its Application in Bioremediation of Soil. *Biodegradation* **2015**, *26* (3), 223–233. <https://doi.org/10.1007/s10532-015-9729-2>.
- (6) Rahkonen, P.; Ettala, M.; Laukkanen, M.; Salkinoja-Salonen, M. Airborne Microbes and Endotoxins in the Work Environment of Two Sanitary Landfills in Finland. *Aerosol Sci. Technol.* **1990**, *13* (4), 505–513. <https://doi.org/10.1080/02786829008959465>.
- (7) Matzke, M.; Jurkschat, K.; Backhaus, T. Toxicity of Differently Sized and Coated Silver Nanoparticles to the Bacterium *Pseudomonas Putida*: Risks for the Aquatic Environment? *Ecotoxicology* **2014**, *23* (5), 818–829. <https://doi.org/10.1007/s10646-014-1222-x>.
- (8) Mallevre, F.; Alba, C.; Milne, C.; Gillespie, S.; Fernandes, T. F.; Aspray, T. J. Toxicity Testing of Pristine and Aged Silver Nanoparticles in Real Wastewaters Using Bioluminescent *Pseudomonas Putida*. *Nanomaterials* **2016**, *6* (3). <https://doi.org/10.3390/nano6030049>.
- (9) Yang, X.; Li, J.; Liang, T.; Ma, C.; Zhang, Y.; Chen, H.; Hanagata, N.; Su, H.; Xu, M. Antibacterial Activity of Two-Dimensional MoS<sub>2</sub> Sheets. *Nanoscale* **2014**. <https://doi.org/10.1039/c4nr01965b>.
- (10) Kalantar-zadeh, K.; Ou, J. Z.; Daeneke, T.; Strano, M. S.; Pumera, M.; Gras, S. L. Two-Dimensional Transition Metal Dichalcogenides in Biosystems. *Adv. Funct. Mater.* **2015**. <https://doi.org/10.1002/adfm.201500891>.
- (11) Teo, W. Z.; Chng, E. L. K.; Sofer, Z.; Pumera, M. Cytotoxicity of Exfoliated Transition-Metal Dichalcogenides (MoS<sub>2</sub>, WS<sub>2</sub>, and WSe<sub>2</sub>) Is Lower than That of Graphene and Its Analogues. *Chem. - A Eur. J.* **2014**, *20* (31), 9627–9632. <https://doi.org/10.1002/chem.201402680>.
- (12) Chng, E. L. K.; Sofer, Z.; Pumera, M. MoS<sub>2</sub> Exhibits Stronger Toxicity with Increased Exfoliation. *Nanoscale* **2014**, *6* (23), 14412–14418. <https://doi.org/10.1039/c4nr04907a>.